

## **On the Impulsive Failure of Bridge Piers by Hyogo–ken Nanbu Earthquake (Kobe, 1995)\***

by

Keiichiro SONODA\*\* and Harutoshi KOBAYASHI\*\*\*

(Received September 29, 1995)

### **Synopsis**

First, impulsive failure modes of civil engineering structures observed in Hyogo–ken Nanbu Earthquake are described. The observed modes seemed to be caused by a vertical shock incident to the bottom face of structural foundation. Second, numerical simulations are carried out to two models of bridge piers, one is reinforced column–model and the other is steel tube column–model, which severely damaged by the earthquake.

A one–dimensional spring–mass model is used to examine the axial stress response in both column and pile sections under a rectangular pulse–like compressive stress introduced to the bottom face of foundation, and the failure modes obtained are discussed in comparison with those observed at the actually damaged structures.

**Keywords :** Earthquake disaster, Impulsive loadings, Bridge pier failure, Numerical simulation

### **1. Introduction**

On 17th January 1995, a great earthquake hit Awaji and Hanshin area in Hyogo prefecture in Japan. Registering magnitude of the earthquake was M7.2 in the Richter scale, which was not the largest among recent earthquakes in Japan, but it gave so severe and fatal damage to residential buildings and civil engineering structures as to shatter 5,500 or more lives, because the focus of this earthquake was not deep (about 10km below the ground level) and was located near a congested urban district–Hanshin area with high dense population of about 3 millions. Figure 1 shows the ground motions at Kobe University recorded by a seismograph [1]. The maximum acceleration recorded was about 800 gals at Kobe Ocean Meteorological Observatory.

---

\* Presented at Asia–Pasific Conference on Shock and Impact Loads on Structures, Singapore, January 23–24, 1996

\*\* Professor, Department of Civil Engineering

\*\*\* Associate Professor, Department of Civil Engineering

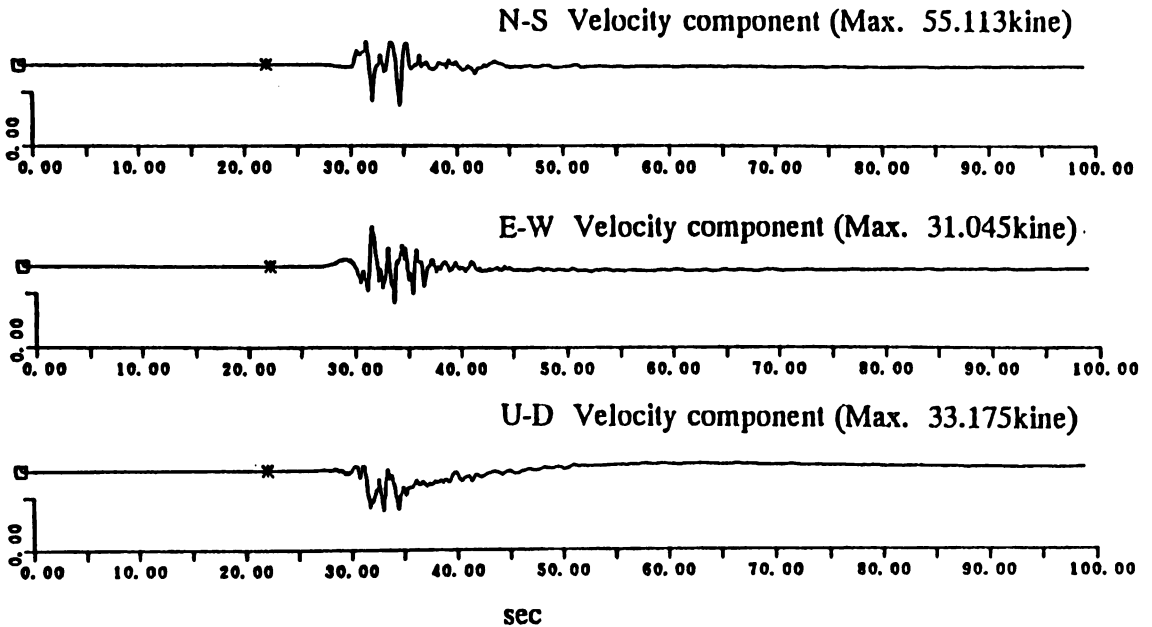


Fig. 1. Strong motion records on a rock site at Kobe University [1]

## 2. Earthquake Impact Forces

Many people living within the meizoseismal region felt a vertical strong shock just before large horizontal shaking. Though such a shock was not observed in the seismographs because of their frequency characteristics, the authors were convinced of the existence of vertical impact force at the earlier stage of the earthquake. Photograph 1 and Figure 2 show the horizontal cracks in the column of a reinforced concrete bridge pier which seemed to be caused by impact tensile forces. Though the cracks of large width are not many, a number of parallel small width cracks can be seen over the whole region of the column. The degree of damage in bridge piers very varies from the earlier stage of only horizontal cracks to the fatal stage of collapse of the column. In the columns suffered from a small damage, some of horizontal cracks were only seen, but in the columns damaged more, the axial reinforcing bars buckled by the repeated action of compressive forces after the tensile cracks occurred and the concrete cover flew out (see Photo. 2). On the other hand, some of steel tube bridge piers buckled by undergoing a strong axial compressive force. For example, Photo. 3 shows a buckling mode for circular steel tube piers. In these damaged piers, an appreciable horizontal deformation of the columns was not seen, it is therefore considered that the vertical impact forces at the earlier stage of earthquake is a main factor to lead the fatal damage of the columns by an additional horizontal shaking.

### 3. Input of Earthquake Impact Force

What is the mechanism of earthquake impact forces? Now, we have no clear answer to this question, but we would like to discuss the input impact force characteristics, considering that a phenomenon of strong vertical shock many people felt at the earlier stage of the earthquake is an evidence of impact forces introduced to the foundation of bridge piers.

As a lot of earthquake engineers and scientists have already pointed out, it is well known that Hyogo-ken Nanbu earthquake was caused by the movement of active faults. Since a typical impact force is produced by collision of two bodies, it seems to be possible that a phenomenon similar to a collision occurred by thrusting the foundation of bridge pier by the action of body waves discharged from active faults.

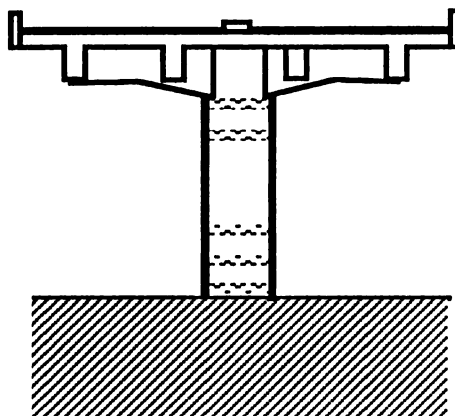


Fig. 2. Sketch of parallel cracks due to impulsive forces in bridge R/C pier

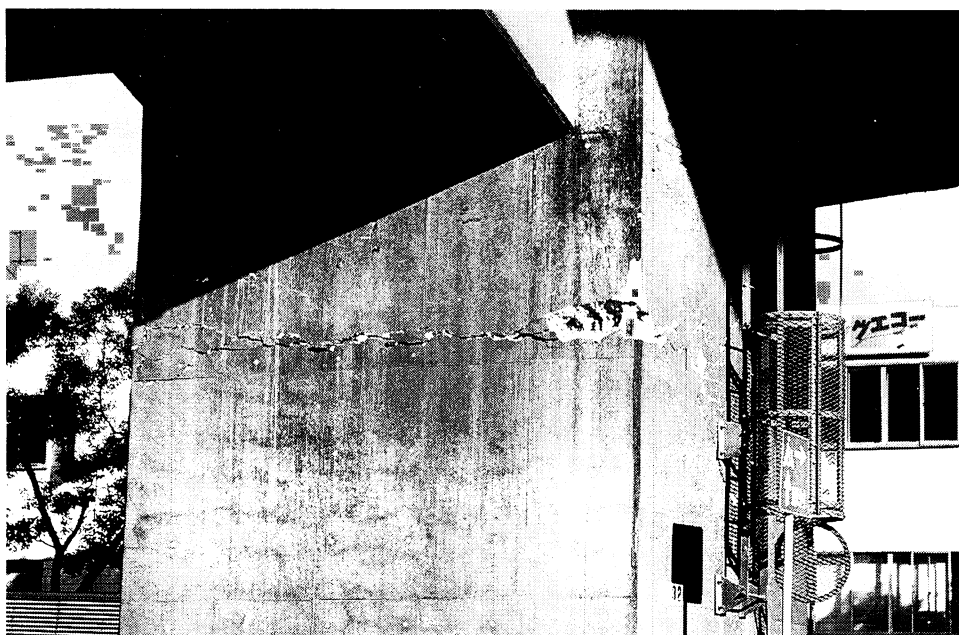


Photo. 1. Tensile failure mode due to impulsive force in a bridge R/C pier



Photo. 2. Compressive failure mode due to impulsive force in a bridge R/C pier

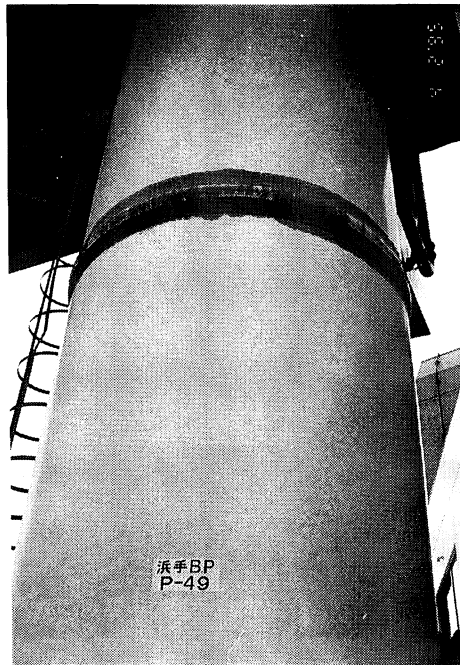


Photo. 3. Buckling mode of circular steel tube bridge pier

Figure 3 shows a schematic figure of ground motion and incident velocity at the bottom end of the foundation of bridge pier. Until the ground velocity attains to its peak value, the foundation of bridge pier has been thrust and the compressive force has increased. When the ground velocity passes its peak value, the compressive force rapidly decreases. After when the total of incident force and self-weight force becomes zero, the foundation of bridge pier bounds upward and afterwards the pier enters in the state of vertical vibration.

If the incident compressive force is smaller than the self-weight force, the pier does not bound and the shape of incident force wave is similar to the incident velocity. Therefore, the following expressions are obtained in a wave modeled by rectangular pulse:

$$t_{d'} = 2t_d, \quad \text{if } \delta_s < \sigma_o$$

$$t_d = t_d \frac{\delta_s + \sigma_o}{\sigma_o}, \quad \text{if } \delta_s < \sigma_o \tag{1}$$

where  $\sigma_s$ =incident compressive stress;  $\sigma_o$ =self-weight compressive stress;  $t_d$ =duration of  $\sigma_s$ ; and  $t_{d'}$ =duration between the peak stress stage and the returning original stress stage.

The incident velocity  $v$  is controlled by the condition of contact between the ground and the bottom face of the foundation of bridge pier. If the ground is soft,  $v$  decreases, while if the ground is hard,  $v$  increases. On the other hand, according to the impact theory of elastic body [2], the relation between the incident velocity and the incident stress is as follows:

$$\sigma_s = - \sqrt{c \rho} v \tag{2}$$

where  $c$ =elastic wave velocity and  $\rho$ =density.

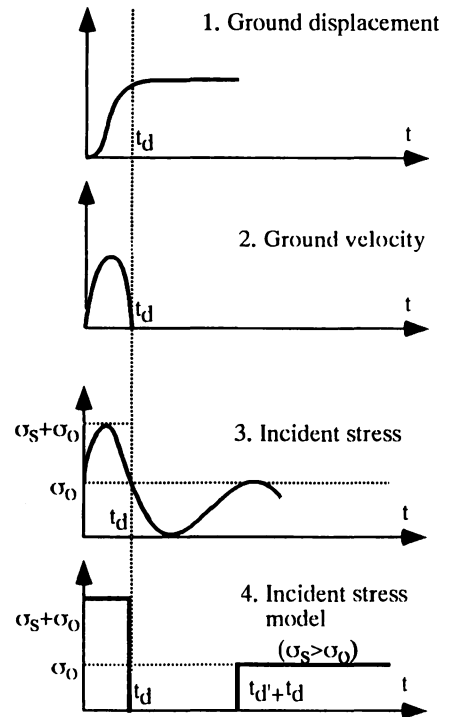


Fig. 3. Ground motion and incident stress

#### 4. Relation of Impulsive Tensile or Compressive Failure and Type of Structures

As mentioned before, since an impact force is produced by collision of two bodies, a soft projectile induces a smaller intensity of impact force than a rigid projectile. Therefore, a structure on a soft ground undergoes a smaller impact force than that on a rigid ground. In fact, in Hyogo–ken Nanbu earthquake, structures with a strong foundation consisting of RC piles or a large concrete caisson supported on a diluvium deposit had suffered from severer damage than those with a weak foundation such as spread foundation.

On the other hand, the reinforced concrete bridge piers and building columns had undergone severer damage than the other members such as slabs and girders in structures. As shown in Fig. 4, the cross sectional area of the column of bridge piers or buildings is

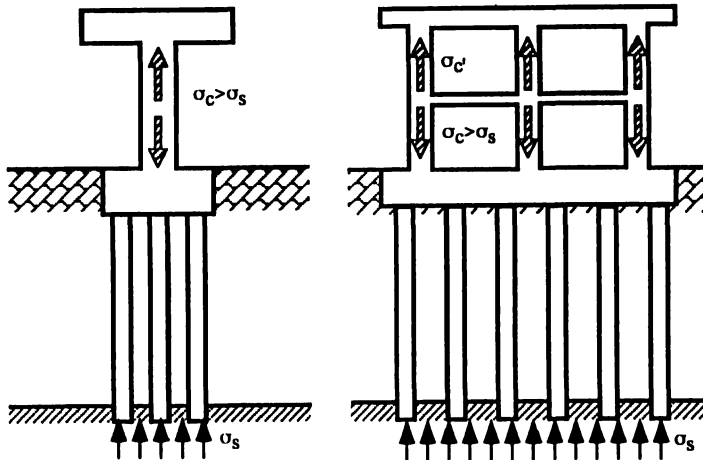


Fig. 4. Amplification of stress in columns

much smaller than the bottom face area of their foundations. Therefore, the intensity of incident stress introduced from the bottom face of foundation enlarges in the section of column. In addition to that, a heavy body of superstructure more increases the stress by the effect of vertical vibration. In consequence, it is concluded that a structure with larger foundation and heavier superstructure undergoes a larger intensity of stress and has more possibility of impulsive failure.

## 5. Numerical Simulations

### 5.1 Reinforced Concrete Bridge Pier

Figure 5(a) shows a reinforced concrete pier and its foundation in a flat slab type bridge which fully collapsed by the earthquake. Here, one-dimensional impact analysis of this structure is carried out using one-dimensional Rigid Body-Spring Model (RBSM) shown in Fig. 5(b). The weight of superstructure is 1,063tf, those of footing and RC piles are 532tf and 452tf, respectively. The material constants of column are as follows: Concrete (Elastic modulus  $E_c=3 \times 10^6 \text{ kgf/cm}^2$ , Density  $\rho_c=2.3 \text{ tf/m}^3$ , Compressive strength  $f_c=300 \text{ kgf/cm}^2$ , Tensile strength  $f_t=30 \text{ kgf/cm}^2$ ); Reinforcing bar (Elastic modulus  $E_s=3 \times 10^6 \text{ kgf/cm}^2$ , Density  $\rho_s=7.85 \text{ tf/m}^3$ , Yield point  $f_{sy}=3,000 \text{ kgf/cm}^2$ ); and Cross sectional area of column and pile (Column:  $A_c=7.5 \text{ m}^2$ , Total of piles:  $A_p=12.6 \text{ m}^2$ ).

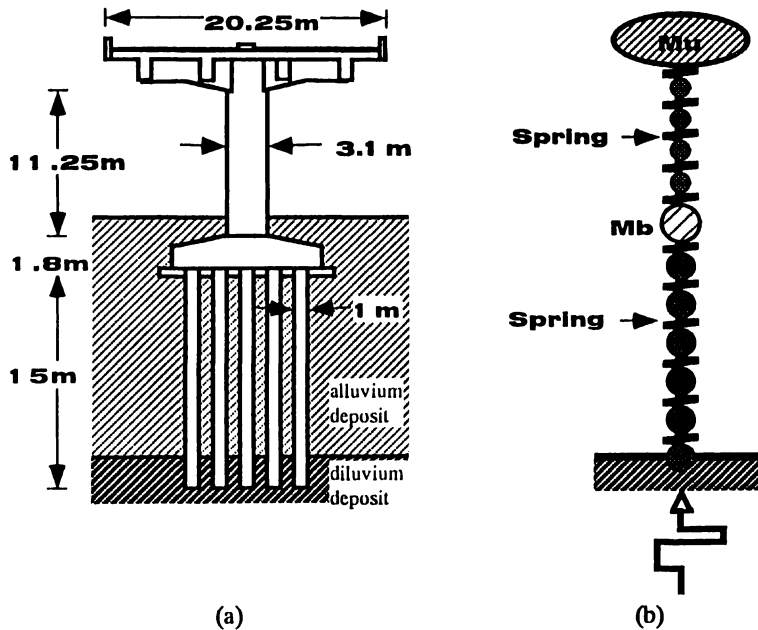


Fig. 5. (a) Bridge model and (b) its numerical model used

### (1) Elastic analysis

Element division used is 20 for the column length (12.5m) and 20 for the pile length (15m). In the first example, incident velocity  $v$  at the bottom of piles is 20cm/s, and duration  $t_d$  of incident compressive stress takes 16ms which is equivalent to double of the time of propagation of an elastic stress wave from the bottom of piles to the top of column. The response of stresses at the top of column and the top of piles are shown in Fig. 6. In this figure, it is seen that the tensile stresses appear in the domain of  $t > t_d$ , and the maximum value occurs at 30ms at the top of column under the effect of vertical vibration with the period of about 33ms. On the other hand, the stress of the top of piles becomes a complicated wave by the effect of repeated reflection of the stress wave within the piles, and the maximum intensity of tensile stress reduces by the effect of larger cross sectional area. In this example, although the incident velocity,  $v$ , is 20cm/s which corresponds to the incident compressive stress,  $13.6\text{kgf/cm}^2$  from Eq. (2), the maximum stresses in the column and the piers attain to several times as large as the incident stress,  $\sigma_s$ .

Next, the effect of duration  $t_d$  of incident compressive stress on the stress response is investigated. Table 1 shows the maximum intensities of tensile and compressive stresses obtained over the whole sections of the column and the piles under the various values of  $t_d$ . When  $t_d$  is smaller than 8ms which corresponds to double of the time of elastic wave propagation from the bottom to the top of piles, the stress intensity of piles becomes greater than that of column by the effect of reflection at the top of piles.

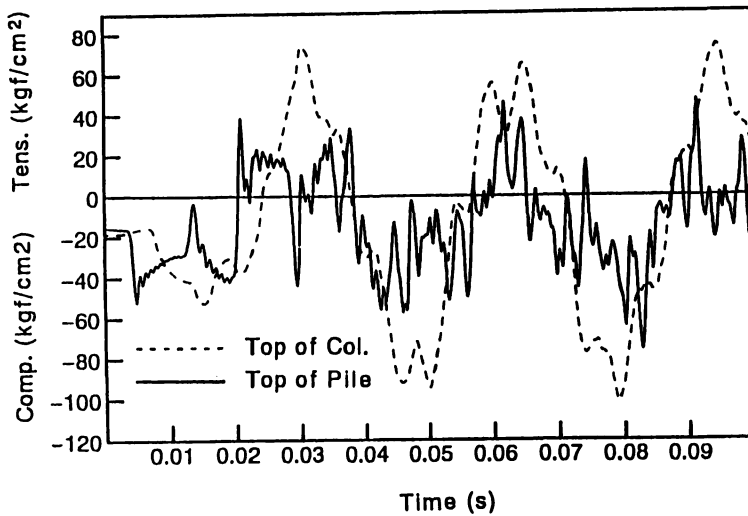


Fig. 6. Stress response at the top of the column or piles ( $v=20\text{cm/s}$  and  $t_d=16\text{ms}$ )

On the other hand, when  $t_d$  is larger than 8ms, the stress intensity of column becomes larger than that of piles. But, even if  $t_d$  is larger than 16ms which corresponds to double of the time of elastic wave propagation from the bottom of piles to the top of column, the stress intensity of column does not increase. Therefore, an increase in  $t_d$  enlarges the magnitude of impulsive and it yields the increase of bounding of foundation, but it does not lead the increase of impulsive force.

Table 1. Maximum tensile and compressive stresses in the column and the piles ( $v=20\text{cm/s}$ )

$t_d(\text{ms})$	Column( $\text{kgf/cm}^2$ )		Piles( $\text{kgf/cm}^2$ )	
	$\sigma_{\max}$	$\sigma_{\min}$	$\sigma_{\max}$	$\sigma_{\min}$
2	16.3	-49.6	49.3	-71.8
4	24.0	-56.2	45.5	-79.2
8	58.1	-88.8	67.1	-103.6
16	74.6	-103.7	44.2	-73.4
32	47.9	-54.0	58.8	-90.6
64	37.0	-51.5	50.3	-62.9
128	46.3	-56.2	52.5	-91.6



(2) Elasto-plastic fracture analysis

Stress-strain relation of the material used in the numerical simulation is shown in Fig.7. It is assumed that coefficient  $\alpha$  takes 10 in the figure and concrete enters in the state of cracking when the tensile strain is over  $1 \times 10^{-3}$ , considering a tension stiffening in concrete, and concrete crushes when compressive strain is over  $3.5 \times 10^{-3}$ .

Figure 8 shows the results obtained in cases of (1)  $v=1\text{m/s}$  and  $t_d=16\text{ms}$  and (2)  $v=2\text{m/s}$  and  $t_d=16\text{ms}$ . The abscissa shows positions of the cross sections of column and piles, namely left point 0 means the bottom of piles, point 20 the top of piles, 21 the bottom of column, and right point 40 the top of column.

In case of  $v=1\text{m/s}$  and  $t_d=16\text{ms}$ , though the strain intensity exceeding  $\epsilon_t$  occurs on the whole regions of column, their maximum values remain at most  $1.4 \times 10^{-3}$ , but the piles remain less than  $\alpha \epsilon_t$ . While, in case of  $v=2\text{m/s}$  and  $t_d=16\text{ms}$ , both the column and the piles cracked, and the maximum intensity of strain appears at the top of column or piles and their values attain to  $4-7 \times 10^{-3}$ . This stage seems to correspond to an actually damage stage of a column with a lot of parallel tensile cracks.

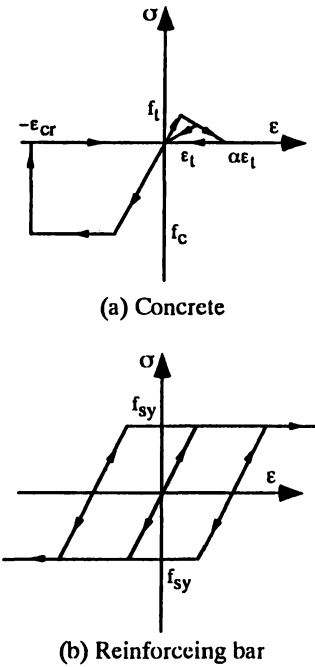


Fig. 7. Stress-strain relation

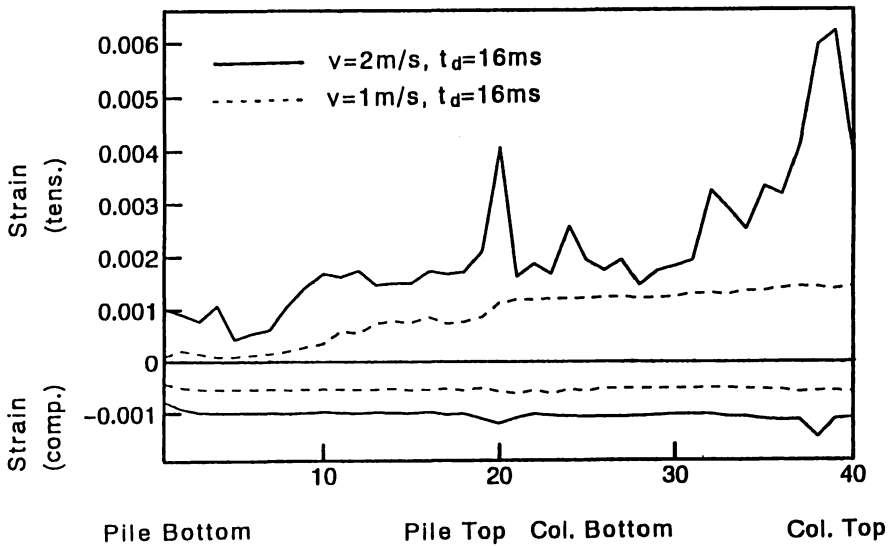


Fig. 8. Maximum tensile or compressive strain envelope

5.2. Circular Steel Bridge Pier

The second example is devoted to examine a buckling of circular steel tube bridge pier observed at the site as shown in Photo. 3. The structural details of this pier are shown in Fig. 9. The pier supports the total weight, 1,480tf, of double deck girders. Thickness of the circular steel tube column of diameter 3.2m varies from 26mm on the upper third, through 30mm on the middle third, to 34mm in the lower third. The buckling shown in Photo. 3 occurred at the bottom of the upper third. For numerical simulation, it is assumed that both the reinforced concrete piles of 26m deep and the rectangular steel tube of superstructure of 12m long are of an elastic material and the circular steel tube column of 12m long, being relevant here, follows the constitutive law shown in Fig. 10 which is modeled according to static buckling test results given in Ref. [3]. In the constitutive relation of Fig. 10, the column behaves as a perfect plastic material before buckling but after buckling it behaves as an unstable material with a residual small resistance, and the descend slope in the stress-strain curve in the unstable domain is determined so as to yield an equivalent dissipative energy after buckling to that obtained by static plastic buckling tests [3,4]. Here, a one dimensional Rigid Body-Spring Model (RBSM) being the same to the first example is used. The number of element division takes 30 for the circular tube column, 10 for the rectangular tube of superstructure and 10 for the piles. The material constants used for concrete are the same to the first

example, and those for the circular steel column are as follows: Elastic modulus  $E_s=2.1 \times 10^6$  kgf/cm<sup>2</sup>; Density  $\rho_s=7.85$ tf/m<sup>3</sup>; and Yield point  $f_{s,y}=3,000$ kgf/cm<sup>2</sup>. Coefficients in the stress-strain model of Fig.10 are  $\alpha=0.3$ ,  $\beta=10$  and  $70 < \gamma < 700$ , where the value of  $\gamma$  depends on the length of element used in RBSM.

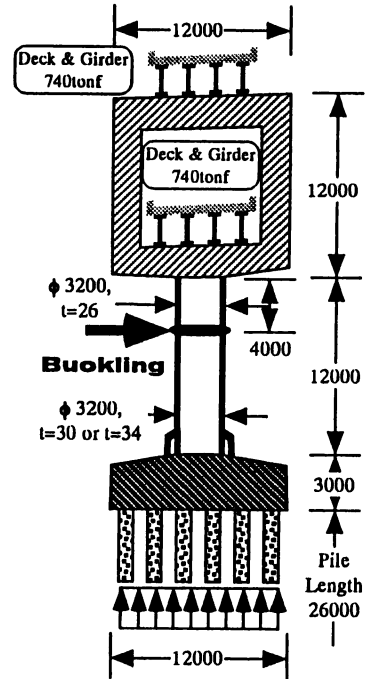


Fig. 9. Structural details of steel bridge pier

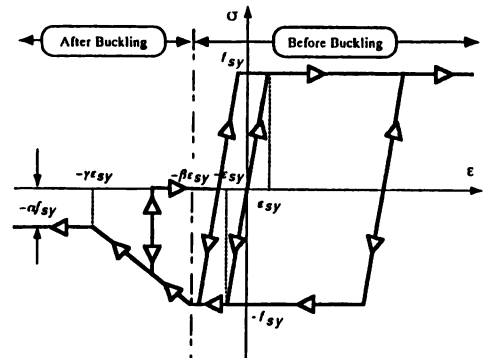


Fig. 10. Constitutive relation for circular steel tube

Figure 11 shows the maximum strain distribution along the column indicated by positions 1–10, the column by 10–40 and the tube of superstructure by 40–50 under the incident velocity  $v=1\text{m/s}$  at the bottom faces of piles and various duration  $t_d$  of the incident stress. From the Figure, it can be known that under a smaller  $t_d$  than 16ms that means a smaller impulsive introduced at the bottom face of piles, no plastic buckling occurs, that means the maximum compressive strain being less than  $\beta \varepsilon_{sv}$ , but under a larger  $t_d$  than

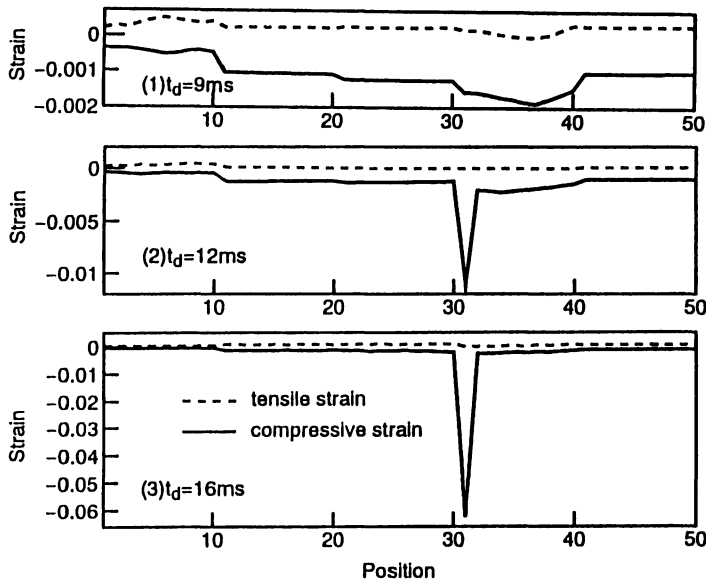


Fig. 11. Maximum strain distributions along column in  $v=1\text{m/s}$

16ms, a buckling occurs in only one element located at the bottom of the upper third of column that is the same position to that observed at the site as shown in Photo. 3. Further, it should be noted that an almost same buckling mode is also obtained, even if the descend slope,  $\gamma$ , varies from 70 to 700 for the unstable domain of the stress–strain relation in Fig.10.

## 6. Concluding Remarks

In Hyogo–ken Nanbu earthquake, a lot of phenomena of bound of bodies such as stone and rock mass on the ground, bridge girders and shoes on a pier have been reported. Such phenomena can not be explained by an ordinal seismic response analysis based on the acceleration wave of a seismograph because it is a kind of impulsive phenomenon. An impulsive phenomenon is a transition phenomenon occurring at the initial stage of earthquake. Though an impulsive wave was not recorded in any of seismograph, this paper has been developed considering a strong vertical shock many people felt as an evidence of vertical impulsive force.

Since an impulsive failure problem of bridge structures has not been enough investigated yet now, we hope that this paper is available to more discuss this problem.

## 7. References

1. Strong Motion Records of Hanshin–Awaji Earthquake Disaster 1995 by The C.E.O.R.K.A.(1995).
2. W. Johnson (1972) Impact Strength of Materials, Edward Arnold, London.
3. N. Jones (1989) Structural Impact, Cambridge Univ. Press, London.
4. K. Murase and N.Jones (1993) Experiments on the dynamic axial plastic buckling of circular tubes, Journal of Society of Material Sciences, Japan, **42**(483)1420–1426.